8-1-2014

# The Geocoronal H α Cascade Component Determined from Geocoronal H β Intensity Measurements

F. L. Roesler
*University of Wisconsin - Madison*

E. J. Mierkiewicz
*Embry-Riddle Aeronautical University*, mierkiee@erau.edu

S. M. Nossal
*University of Wisconsin - Madison*

AGU PUBLICATIONS

JGR

Journal of Geophysical Research: Space Physics

RESEARCH ARTICLE
10.1002/2014JA020026

**Key Points:**
- Geocoronal H-α and H-β measurements are used to determine H-α cascade
- Cascade accounts for measured red wing enhancement of the H-α airglow
- H-line profiles with cascade improve measured exospheric velocity distributions

**Correspondence to:**
S. M. Nossal,
nossal@physics.wisc.edu

**Citation:**
Roesler, F. L., E. J. Mierkiewicz, and S. M. Nossal (2014), The geocoronal H α cascade component determined from geocoronal H β intensity measurements, *J. Geophys. Res. Space Physics*, *119*, 6642–6647, doi:10.1002/2014JA020026.

Received 28 MAR 2014
Accepted 2 JUL 2014
Accepted article online 5 JUL 2014
Published online 1 AUG 2014

# The geocoronal H α cascade component determined from geocoronal H β intensity measurements

**F. L. Roesler[1], E. J. Mierkiewicz[2], and S. M. Nossal[1]**

[1]Department of Physics, University of Wisconsin-Madison, Madison, Wisconsin, USA, [2]Department of Physical Sciences, Embry-Riddle Aeronautical University, Daytona Beach, Florida, USA

**Abstract** Geocoronal H α and H β intensity measurements using the Wisconsin H α Mapper Fabry-Perot are used to determine the intensity of the H α cascade component. From basic atomic physics and the work of Meier (1995), we show that the total cascade in geocoronal H α emission is 0.52 ± 0.03 times the geocoronal H β intensity, *I*(H β), for solar Lyman series excitation of geocoronal hydrogen. The results are consistent with the H α cascade measurements of Mierkiewicz et al. (2012), which were determined directly from the analysis of H α line profile measurements, and significantly narrow the range of uncertainty in the cascade measurement. Accounting for cascade is essential in determining exospheric effective temperatures and dynamics from the shape of the geocoronal H α line.

## 1. Introduction

The first measurements of geocoronal Balmer alpha (H α) and Balmer beta (H β) at high enough resolving power to separate galactic and terrestrial contributions were made by *Reynolds et al.* [1973] using a scanning 150 mm aperture Fabry-Perot spectrometer of very low sensitivity by modern standards. Since then, improvements in Fabry-Perot spectroscopy, particularly the advent of Fabry-Perot (FP)/charge-coupled device (CCD) annular summing in which a highly sensitive charge-coupled device (CCD) camera is used to image multiple annular Fabry-Perot (FP) ring elements [*Coakley et al.*, 1996], have increased sensitivities by more than 2 orders of magnitude. Furthermore, accurate calibration sources have been established [*Scherb*, 1981; *Madsen and Reynolds*, 2005]. The advances led to the development of the highly sensitive Wisconsin H α Mapper (WHAM) facility [*Haffner et al.*, 2003] that is capable of making high-precision measurements of very faint night-sky emission lines. We have made near-simultaneous intensity measurements of geocoronal H α and H β with WHAM while targeting look directions that minimize galactic background contamination. The results are discussed below in the context of determining the cascade contribution to the geocoronal H α line profile and intensity.

The first published discussion of the effect of cascade on the geocoronal H α emission line profile appears to be in a paper by *Chamberlain* [1987], in which he points out that measurements of H β intensities would provide a measurement of a cascade component that might explain the small red wing enhancement seen in H α line profiles by *Yelle and Roesler* [1985]. The cascade contribution to H α was examined by *Meier* [1995] in his study of the effect of solar Lyman series line profiles and intensities on geocoronal hydrogen excitation rates. *Nossal et al.* [1998] used the Pine Bluff, Wisconsin Fabry-Perot with the photomultiplier replaced with a CCD, converting it to an annular summing spectrometer, to make high-resolution measurements of geocoronal H α line profiles. The profiles were fit with two clusters of lines, one for the components from direct solar excitation to $n = 3$ and another for the components from cascade with relative intensities from Meier's study [*Meier*, 1995]. Results in rough agreement with Meier's prediction of about 7% cascade were obtained. Meier later revised his estimate to 4.5% (R. R. Meier, private communication, 1998) based on new solar Lyman series intensities by *Warren et al.* [1998].

*Mierkiewicz* [2002] rebuilt the Pine Bluff Fabry-Perot to optimize it for the FP/CCD technique at a resolving power of 80,000 [*Mierkiewicz et al.*, 2006] and obtained an extensive data set of well-calibrated H α line profiles. WHAM maps of galactic H α background intensities and velocity distributions [*Haffner et al.*, 2003] were used to select look directions that minimized distortions of the geocoronal line profiles due to galactic contamination. The result for the cascade component to H α was 5 ± 3%, where the error range is predominantly data scatter [*Mierkiewicz et al.*, 2012].

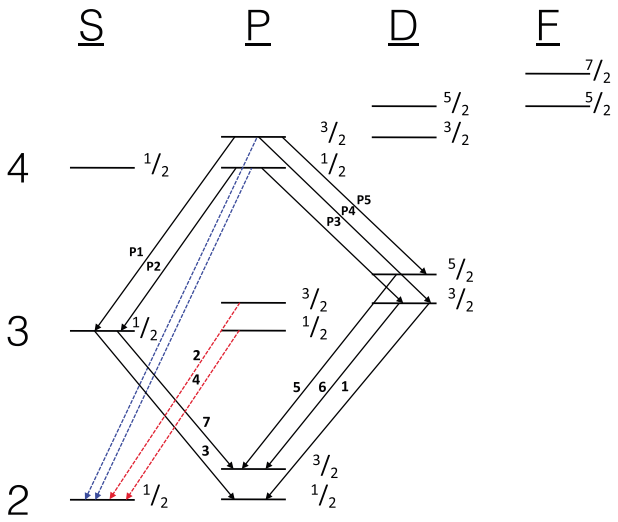


**Figure 1.** Hydrogen energy level diagram. The directly excited H β and H α transitions are indicated with blue and red lines, respectively. The Paschen transitions are marked with Ps. The H α emission components are numbered. Components 1, 3, 5, 6, and 7 are the cascade components; components 2 and 4 are from direct solar excitation. (H α line component positions are indicated in Figure 3).

Accounting for the cascade excitation is important for the isolation of possible dynamical signatures in the line profile [*Yelle and Roesler*, 1985], the retrieval of the exospheric effective temperature [*Mierkiewicz et al*., 2012; *Nossal et al*., 1998], the reduction in uncertainties in the hydrogen column emission intensity used in forward modeling retrievals of geophysical parameters [*Bishop et al*., 2004], and the improved accuracy of climatology comparisons [*Nossal et al*., 2008].

## 2. H β Intensity and H α Cascade

Geocoronal H β arises predominantly from solar Lyman gamma (Ly γ) excitation to the $n = 4$ levels of geocoronal hydrogen (Figure 1). From the ground state of H, only the $4^2P$ levels are excited by direct solar radiation. These decay partly to the $2^2S$ levels producing the H β line. Other decay channels are to the $3^2S$ and $3^2D$ levels, giving rise to the Paschen alpha line. The $3^2S$ and $3^2D$ levels subsequently can decay only to the $2^2P$ levels, producing the cascade components of H α; thus, the cascade rate is equal to the Paschen alpha rate. Referring to Figure 1, the lines marked P1 and P2 are the 4p-3s Paschen transitions; P3, P4, and P5 are the 4p-3d Paschen transitions; and H β1 and H β2 are the 4p-2s transitions, giving rise to H β, which we measure. In terms of the transition probabilities $A_{ki}$ (upper level $k$ to lower level $i$) from Table B for hydrogen in the NBS tables of atomic transition probabilities [*Wiese et al*., 1966], the cascade rate for H α is $A_{ki}(4p\text{-}3s) + A_{ki}(4p\text{-}3d) = 3.065 \times 10^6\ s^{-1} + 3.475 \times 10^5\ s^{-1}$, and the H β rate is $A_{ki}$ (4p-2s) $= 9.67 \times 10^6\ s^{-1}$.

The H α cascade component relative to H β is thus

$$[A_{ki}(\mathrm{P1} + \mathrm{P2}) + A_{ki}(\mathrm{P3} + \mathrm{P4} + \mathrm{P5})] / A_{ki}(\mathrm{H}\ \beta 1 + \mathrm{H}\ \beta 2) = 0.353 \quad (1)$$

This gives a cascade contribution to H α of $I$(cascade) = 0.353 $I$(H β), for intensities measured in photon emission rates such as rayleighs:

$$\left(1\ \mathrm{R} = \frac{10^6}{4\pi}\ \mathrm{photons\ s^{-1}cm^{-2}sr^{-1}}\right)$$

The relative intensities and positions of the cascade components were addressed by *Meier* [1995] (Table 3 and Figure 9 therein) and by *Nossal et al*. [1998] (Figures 2 and 3 therein). In accord with their work, the calculation here shows that 90% of the cascade goes into components 7 and 3: that is $A_{ki}$ (P1 + P2)/($A_{ki}$ (P1 + P2) + $A_{ki}$ (P3 + P4 + P5)) = 0.90. Components 7 and 3 are distributed in a 2:1 intensity ratio. Thus, 60% of the cascade appears in component 7, that is, more than a full width at half maximum to the red of the center of gravity of the directly excited H α line. Thus, cascade can readily account for the measured red wing enhancement of H α emission as observed by *Yelle and Roesler* [1985], *Nossal et al*. [1998], and *Mierkiewicz et al*. [2012]. (Line component positions are indicated in Figure 3 below).

## 3. Adjustment for Cascade From $N > 4$

While most of the cascade in geocoronal H α is that calculated above from $n = 4$ alone, there is an additional cascade from solar excitation to the P levels for $n > 4$. *Meier* [1995] has calculated the

cascade contribution to the $3^2S$ and $3^2D$ parent states for H α from all higher quantum numbers using branching ratios and measured solar excitation rates. Meier's calculated cascade contributions can be used to estimate a better value for the total cascade contribution to *I*(H α) based on the actual measurement of *I*(H β).

Reading values for the product of the excitation *g* factors and the total branching ratios from Figure 7 in *Meier*'s [1995] paper, we determine a value proportional to $1.85 \times 10^{-8}\,s^{-1}$ for cascade to $3^2S$ and $0.21 \times 10^{-8}\,s^{-1}$ for cascade to $3^2D$ from Ly γ excitation to $4^2P$. For the sum of cascades to $n = 3$ from all levels $n = 4$ and higher, we determine a value proportional to $2.70 \times 10^{-8}\,s^{-1}$ to $3^2S$ and $0.28 \times 10^{-8}\,s^{-1}$ to $3^2D$. The cascade from $n = 4$ is thus a fraction $(1.85 + 0.21)/(2.70 + 0.28) = 0.69$ of the total cascade to $n = 3$. This yields an improved H α cascade intensity of (0.353/0.69) *I*(H β) = 0.51 *I*(H β), where *I*(H β) is the measured H β intensity.

Revised data provided by Meier [private communication, 1998] based on the *Warren et al*. [1998] solar Lyman line measurements show an excitation *g* factor for $n = 3$ the same as in his 1995 paper, while the revised *g* factor for $n = 4$ is lower by a factor 0.63. This is the main reason for the reduction in Meier's calculation for the H α cascade: $7.1\% \times 0.63 = 4.5\%$. We have repeated the above calculation for estimating the cascade from $n > 4$ using Meier's revised data, assuming excitation *g* factors for $n > 10$, with ratios the same as the average of those he provided for $n = 4$ through $n = 10$. The fraction of cascade from all $n > 4$ relative to cascade from $n = 4$ is found to have a value of 0.673. This yields a factor 0.53 for the fraction of the measured H β intensity that gives the H α cascade component. Two small factors are not included in determining our results: the $3^2P$-$2^2S$ cascade of about 0.1% of the H α intensity [*Meier*, private communication, 1998] and the cascade component of a few percent in the H β intensity [*Meier*, 1995]. Provisionally, we adopt the value for the H α cascade intensity of $0.52 \pm 0.03$ *I*(H β), with the error estimate chosen to bracket both calculated values and any H β cascade.

Note that for the cascade from $n > 4$, 90% goes to $3^2S$ and 10% goes to $3^2D$, similar to the ratio found above for the 4–3 transitions: thus, the cascade relative intensities to $n = 2$ are unchanged when the additional cascade from $n > 4$ to $3^2S$ and $3^2D$ is included. We again find that the red wing component 7 has 60% of the cascade intensity into H α, thus giving component 7 a total cascade intensity of 0.31 *I*(H β).

We adopt these cascade results as good working values pending refined modeling and more observations. As Meier pointed out in the conclusions to his 1995 paper, it is not known how Lyman series line center fluxes vary with solar activity, and the effects of multiple scattering of the Lyman series lines in a realistic hydrogen atmosphere were not included in his work. *Meier*'s [1995] work was based on solar Lyman line measurements made in 1962 at low solar activity. Our H α and H β measurements shown in Figure 2 were made during solar minimum in 2008, while the cascade determinations from line profiles of *Mierkiewicz et al*. [2012] were made using data from 2000 during solar maximum. We conclude from the nominal agreement of these different methods of cascade measurement that the cascade fraction of the H α intensity is not strongly dependent on solar cycle phase. However, the uncertainty in determining cascade from the profiles [*Mierkiewicz et al*., 2006, 2012] is larger than the determination from simultaneous H α and H β measurements, as described in section 5 below. Measurements of the behavior of H α and H β over a solar cycle can be expected to lead to more accurate determination for cascade. This will also provide information about the relative solar cycle variation of solar Lyman series line center fluxes.

## 4. H α and H β Intensity Measurements

Figure 2 illustrates near-coincident observations of the H α and H β column emission intensity taken by the Wisconsin H α Mapper (WHAM) Fabry-Perot on the nights of 2 February, 6 March, and 10 March 2008. The WHAM instrument is a double-etalon annular summing Fabry-Perot interferometer coupled to a pointing and tracking siderostat, then located at the Kitt Peak, AZ, observatory [*Haffner et al*., 2003; *Mierkiewicz et al*., 2006]. The observations used in this study were taken pointed toward regions of the sky with low-galactic hydrogen emission. Observations were made alternating between H α and H β. Calibration of the H α line was tied to a 1° patch of the North American Nebula with intensity 800 *R* ± 10% [*Haffner et al*., 2003]. The H β intensity calibration for the same patch of the North American Nebula is

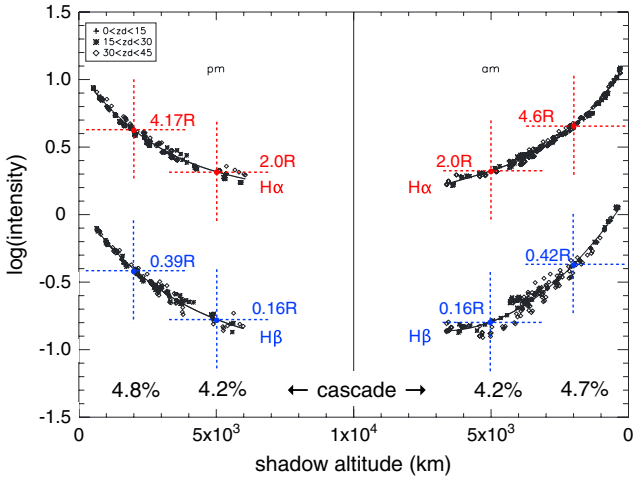


**Figure 2.** Observations of the H α and H β intensities taken by the Wisconsin H α Mapper Fabry-Perot on the nights of 9 February, 6 March, and 10 March 2008. The log of the intensities in rayleighs is plotted versus shadow altitude, because the H α intensity is roughly 10 times brighter than the H β intensity for a given shadow altitude. Sample cascade calculations are shown using H α and H β intensity values for shadow altitudes of 2000 km and 5000 km premidnight and post midnight, as marked by the large red and blue crosses. Note the expected downward trend in the relative cascade emission with increasing shadow altitude.

157 $R \pm 10\%$ and is that used by *Madsen and Reynolds* [2005]. The H α/H β ratio is well determined (G. J. Madsen, private communication, 2013), with the absolute uncertainty determined by the absolute uncertainty in the original H α calibration.

## 5. Cascade Determinations From Data

In Figure 2, intensities are shown on a log scale so the behavior of both lines, along with their excellent precision, can be clearly seen even though geocoronal H α intensities are roughly 10 times brighter than H β intensities. Highlighted on the figure, for the purpose of illustrating the point of this paper, are intensity values for shadow altitudes of 2000 km and 5000 km premidnight and postmidnight. For example, at 2000 km shadow altitude premidnight, $I$(H α) = 4.17 $R$ and $I$(H β) = 0.39 $R$. Following the above procedure, H α cascade is 0.52 $I$ (H β) = 0.20 $R$. In relative terms as used by *Meier* [1995], *Nossal et al*. [1998], and *Mierkiewicz et al*. [2012] in their studies, that becomes 4.8% of $I$(H α). This is consistent with the value of 5 ± 3% determined by *Mierkiewicz et al*. [2012] from H α line profile measurements and with Meier's revised value of 4.5%. As noted above, 60% of the cascade intensity is in the red wing component 7; thus, its intensity is 0.12 $R$, or 2.9% of the total intensity determined for H α, an amount readily detected in modern high-resolution H α line profile measurements. (Note: WHAM has insufficient resolving power to measure profile details). Other values on Figure 2 are determined in a similar way.

In Figure 2, note that the behavior with shadow altitude for H α and H β is different, with H α falling less rapidly with increasing shadow altitude than H β: this is expected because multiple scattering in geocoronal hydrogen for Lyman β (Ly β) is greater than for Ly γ. Thus, there is a trend for the cascade to become a smaller fraction of the H α intensity at larger shadow altitudes. The resulting change in cascade contribution with shadow altitude is not obvious in cascade determination from line profiles because of the rather large uncertainty [*Mierkiewicz et al*., 2006]. Lyman excitation for $n > 4$ will also vary with shadow height. The effect of multiple scattering was not considered in Meier's calculation.

Finally, in Figures 3a and 3b, we present a model line profile for the H α line using well-determined effective temperature measurements for geocoronal hydrogen [*Mierkiewicz et al*., 2012] and the cascade results based on H α and H β intensity measurements from this paper (the effective temperature is that determined by Gaussian fitting to the observed line profiles which are not strictly Gaussian). The model profile is based on an effective temperature of ~800 K (6 km/s full width at half maximum) and a cascade emission that is 5% of the total emission. These conditions are typical for shadow heights of 1000 km in the March time frame [*Mierkiewicz et al*., 2012]. The directly excited emissions are those labeled 2 and 4, and the cascade emission is along fine-structure paths 1,3,5,6, and 7. In Figure 3b, the ordinate is changed to facilitate seeing the cascade emission contributions more clearly. The centroid positions of the fine-structure components are included on the top of the plot with zero at the location of component 4. Note that components 7 and 3 contain 90% of the cascade and that components 1, 5, and 6 are too faint to be easily seen on these figures (see *Nossal et al*. [1998] for more details). The majority of the cascade-excited emission is on the red wing of the line profile as illustrated in Figures 3a and b.

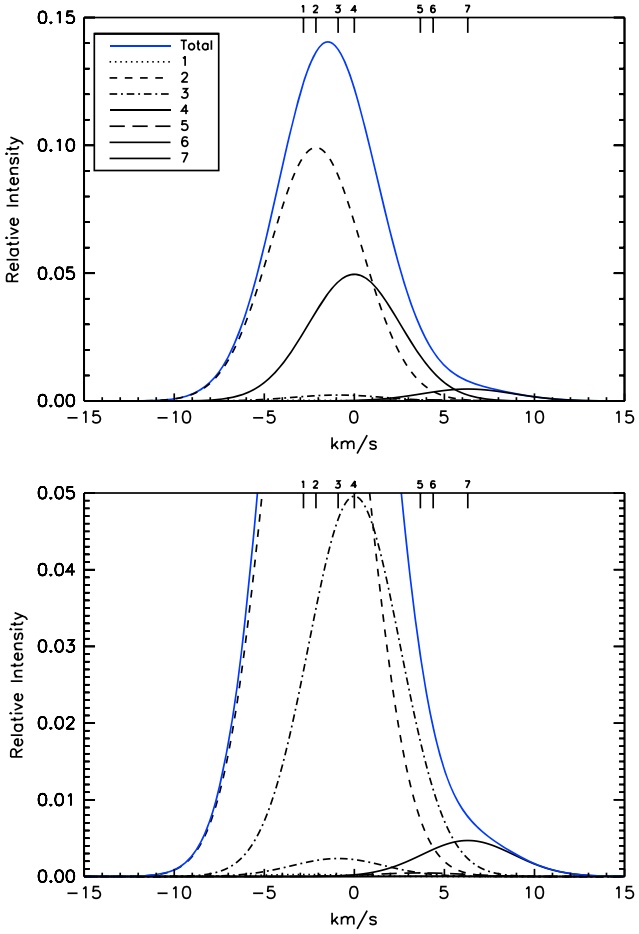


**Figure 3.** (a) A model line profile for the H α line that uses an effective temperature of ~800 K (6 km/s full width at half maximum) and a cascade emission that is 5% of the total emission (see text for more details). The directly excited emissions are those labeled 2 and 4. The cascade emission is along fine-structure paths 1, 3, 5, 6, and 7. Note that components 7 and 3 contain 90% of the cascade and that components 1, 5, and 6 are too faint to be easily seen on these figures. This figure illustrates that the majority of the cascade-excited emission is on the red wing of the line profile. The centroid positions of the fine-structure components are included on the top of the plot with zero at the location of component 4. (b) Same as Figure 3a except that the ordinate has been expanded to more clearly show the cascade-excited emission fine structure.

## 6. Conclusions

This paper conclusively demonstrates the occurrence of cascade excitation in geocoronal H α emission and provides a method independent of line profile measurements for determining H α cascade. Using atomic transition probabilities and the calculations by Meier of the contributions for cascade from $n \geq 4$, we determine the H α cascade intensity from the measured H β intensity. The values of the H α cascade emission calculated here from H β are within the values measured using line profile fitting by *Mierkiewicz et al.* [2012] and significantly narrow the range of uncertainty in the cascade measurement. There is insignificant error in the factor of 0.353 determined from quantum mechanics in section 2, but the adjustment factor found in section 3 depends on ratios of the measured solar Lyman lines for $n > 4$. We expect ratios to have higher accuracy than the absolute intensities and have used the ratios both from Meier's original and revised works to estimate the provisional factor and uncertainty used to determine H α cascade. We believe that our work advances the cascade issue significantly and opens pathways to future advances in modeling and observational studies related to geocoronal hydrogen.

Accounting for cascade is essential for accurate retrieval of the exospheric effective temperature determined from the Doppler width of the profile. Neglect of cascade can lead to overestimates of the retrieved exospheric effective temperature by as much as 100–200 K [*Nossal et al.*, 1997, 1998]. The cascade contribution was included in the fits to the *Mierkiewicz et al.*'s [2012] line profile measurements that demonstrated a semiannual variation in the exospheric effective temperature near the exobase.

In a search for line profile features peculiar to exospheric dynamics [see for example, *Bishop and Chamberlain*, 1987], inclusion of the cascade-excited H α emission is crucial for the accurate analysis of the H α line profile. Signatures of excitation mechanisms, such as charged particle excitation [see for example, *Bishop et al.*, 2001], that would excite all fine-structure components in intensity ratios distinct from solar excitation, would most easily be detected as wing enhancement, predominantly on the red side of the profile, because of the enhancement they would produce in components 1, 5, 6, and 7 [see for example, *Series*, 1957]. Cascade, if very well determined from H α and H β intensity measurements, can be subtracted from precise profile measurements to improve the possibility of extracting dynamical information beyond effective temperatures from the profiles. Our measurements [*Mierkiewicz et al.*, 2012; *Yelle and Roesler*, 1985] suggest that at

midlatitudes, excitation, other than solar Lyman line excitation and cascade, is very small; any presence might be falsely interpreted as small effective temperature changes.

In addition to cascade, serious analysis challenges to interpretation of line profiles come from the ubiquitous galactic H α and H β background and faint airglow lines [*Haffner et al*., 2003; *Madsen and Reynolds*, 2005; *Hausen et al*., 2002]. In combination, these features obfuscate the extraction of physics from geocoronal H α line profile measurements. However, much progress has been made in understanding and accounting for background sources of emission. With the application of highly sensitive and precise instrumentation used in carefully designed observational programs at good observing sites, further progress can be anticipated in this area.

**Acknowledgments**
The authors thank D. Gardner for his assistance with figures and L M. Haffner for the collaborative use of the Wisconsin H α Mapper Fabry-Perot. Please contact the authors for free access to the observational data. This work was supported by the National Science Foundation through awards AGS-1347687, AGS-0940270, AGS-0836367, and AST-1108911.

Michael Liemohn thanks Robert Meier and another reviewer for their assistance in evaluating this paper.

## References

Bishop, J., and J. W. Chamberlain (1987), Geocoronal structure: 3. Optically thin, Doppler-broadened line profiles, *J. Geophys. Res.*, *92*(A11), 12,389–12,397, doi:10.1029/JA092iA11p12389.

Bishop, J., J. Harlander, S. Nossal, and F. L. Roesler (2001), Analysis of Balmer α intensity measurements near solar minimum, *J. Atmos. Sol. Terr. Phys.*, *63*, 341–353.

Bishop, J., E. J. Mierkiewicz, F. L. Roesler, J. F. Gomez, and C. Morales (2004), Data-model comparison search analysis of coincident PBO Balmer α, EURD Lyman β geocoronal measurements from March 2000, *J. Geophys. Res.*, *109*, A05307, doi:10.1029/2003JA010165.

Chamberlain, J. W. (1987), Balmer profiles in the geocorona and interstellar space: 1. Asymmetries due to fine structure, *Icarus*, *70*, 476–482.

Coakley, M. M., F. L. Roesler, R. J. Reynolds, and S. Nossal (1996), Fabry-Perot/CCD annular summing spectroscopy: Study and implementation for aeronomy applications, *Appl. Opt.*, *35*, 6479–6493.

Haffner, L. M., R. J. Reynolds, S. L. Tufte, G. J. Madsen, K. P. Jaehnig, and J. W. Percival (2003), The Wisconsin H-alpha mapper northern sky survey, *Astrophys. J.S.*, *149*, 405–422.

Hausen, N. R., R. J. Reynolds, L. M. Haffner, and S. L. Tufte (2002), Interstellar Hα line profiles toward HD 93521 and the Lockman window, *Astrophys. J.*, *565*, 1060–1068.

Madsen, G. J., and R. J. Reynolds (2005), An investigation of diffuse interstellar gas toward a large, low-extinction window into the inner galaxy, *Astrophys. J.*, *630*, 925–944.

Meier, R. R. (1995), Solar Lyman-series line profiles and atomic hydrogen excitation rates, *Astrophys. J.*, *452*, 462–471, with Erratum (1996), *Astrophys. J.*, *468*, 455.

Mierkiewicz, E. J. (2002), Fabry-Perot observations of the hydrogen geocorona, PhD thesis, Univ. of Wis., Madison.

Mierkiewicz, E. J., F. L. Roesler, S. M. Nossal, J. Bishop, R. J. Reynolds, and L. M. Haffner (2006), Geocoronal hydrogen studies using Fabry-Perot Interferometers, Part 1: Instrumentation, observations, and analysis, *JASTP*, *68*, 1520–1552, doi:10.1016/j.jastp.2005.08.024.

Mierkiewicz, E. J., F. L. Roesler, and S. M. Nossal (2012), Observed seasonal variations in exospheric effective temperatures, *J. Geophys. Res.*, *117*, A06313, doi:10.1029/2011JA017123.

Nossal, S., F. L. Roesler, M. M. Coakley, and R. J. Reynolds (1997), Geocoronal hydrogen Balmer-α line profiles obtained using Fabry-Perot annular summing spectroscopy: Effective temperature results, *J. Geophys. Res.*, *102*(A7), 14,541–14,554, doi:10.1029/97JA00293.

Nossal, S., F. L. Roesler, and M. M. Coakley (1998), Cascade excitation in the geocoronal hydrogen Balmer-α line, *J. Geophys. Res.*, *103*(A1), 381–390, doi:10.1029/97JA02435.

Nossal, S. M., E. J. Mierkiewicz, F. L. Roesler, L. M. Haffner, R. J. Reynolds, and R. C. Woodward (2008), Geocoronal hydrogen observations spanning three solar minima, *J. Geophys. Res.*, *113*, A11307, doi:10.1029/2008JA013380.

Reynolds, R. J., F. L. Roesler, and F. Scherb (1973), Low-intensity Balmer emissions from the interstellar medium and geocorona, *Astrophys. J.*, *179*, 651–657.

Scherb, F. (1981), Hydrogen production rates from ground-based Fabry-Perot observations of comet Kohoutek, *Astrophys. J.*, *243*, 644.

Series, G. W. (1957), *Spectrum of Atomic Hydrogen*, Oxford Univ. Press, London, U. K.

Warren, H. P., J. T. Mariska, and K. Wilhelm (1998), High-resolution observations of the solar hydrogen Lyman lines in the quiet Sun with the SUMER instrument on SOHO, *Astrophys. J. Suppl. Ser.*, *119*, 105–120.

Wiese, W. L., M. W. Smith, and B. M. Glennon (1966), *Atomic Transition Probabilities: Volume 1: Hydrogen Through Neon*, National Bureau of Standards, U. S. Government Printing Office, Washington, D. C.

Yelle, R. V., and F. L. Roesler (1985), Geocoronal Balmer alpha line profiles and implications for the exosphere, *J. Geophys. Res.*, *90*, 7568–7580, doi:10.1029/JA090iA08p07568.